Archival Report

Biological Psychiatry

Genetic Ablation of *GIGYF1*, Associated With Autism, Causes Behavioral and Neurodevelopmental Defects in Zebrafish and Mice

Zijiao Ding, Guiyang Huang, Tianyun Wang, Weicheng Duan, Hua Li, Yirong Wang, Huiting Jia, Ziqian Yang, Kang Wang, Xufeng Chu, Evangeline C. Kurtz-Nelson, Kaitlyn Ahlers, Rachel K. Earl, Yunyun Han, Pamela Feliciano, Wendy K. Chung, Evan E. Eichler, Man Jiang, and Bo Xiong

ABSTRACT

BACKGROUND: Autism spectrum disorder is characterized by deficits in social communication and restricted or repetitive behaviors. Due to the extremely high genetic and phenotypic heterogeneity, it is critical to pinpoint the genetic factors for understanding the pathology of these disorders.

METHODS: We analyzed the exomes generated by the SPARK (Simons Powering Autism Research) project and performed a meta-analysis with previous data. We then generated 1 zebrafish knockout model and 3 mouse knockout models to examine the function of *GIGYF1* in neurodevelopment and behavior. Finally, we performed whole tissue and single-nucleus transcriptome analysis to explore the molecular and cellular function of *GIGYF1*.

RESULTS: *GIGYF1* variants are significantly associated with various neurodevelopmental disorder phenotypes, including autism, global developmental delay, intellectual disability, and sleep disturbance. Loss of *GIGYF1* causes similar behavioral effects in zebrafish and mice, including elevated levels of anxiety and reduced social engagement, which is reminiscent of the behavioral deficits in human patients carrying *GIGYF1* variants. Moreover, excitatory neuron–specific *Gigyf1* knockout mice recapitulate the increased repetitive behaviors and impaired social memory, suggesting a crucial role of *Gigyf1* in excitatory neurons, which correlates with the observations in single-nucleus RNA sequencing. We also identified a series of downstream target genes of *GIGYF1* that affect many aspects of the nervous system, especially synaptic transmission.

CONCLUSIONS: De novo variants of *GIGYF1* are associated with neurodevelopmental disorders, including autism spectrum disorder. *GIGYF1* is involved in neurodevelopment and animal behavior, potentially through regulating hippocampal CA2 neuronal numbers and disturbing synaptic transmission.

https://doi.org/10.1016/j.biopsych.2023.02.993

Autism spectrum disorder (ASD) is a group of neurodevelopmental disorders (NDDs) that is defined by early onset of social communication deficits and repetitive or stereotyped behaviors (1). Additionally, some individuals with ASD also exhibit one or more co-occurring symptoms such as intellectual disability, sensory issues, sleep disorders, and gastrointestinal dysfunction (2,3). The global prevalence of ASD worldwide is approximately 1% to 2% (4), and the number of individuals diagnosed has increased steadily over the past 20 years (5). Genetic factors are major causes of ASD, with extremely high genetic heterogeneity and complex genetic architecture (6,7). Recently, large-scale genetic studies have identified multiple risk genes and highlighted the contributions of de novo variants (DNVs) to ASD (8–10).

There is emerging evidence suggesting that DNVs in *GIGYF1* are associated with ASD and related NDDs. Initially, 3 de novo likely gene disruptive (dnLGD) (including stop-gained, frameshift, or splice mutations) variants were identified by exome sequencing of 2508 autism families from the Simons Simplex Collection (11). Another dnLGD variant was identified in 465 ASD trios by the SPARK (Simons Powering Autism Research) pilot project (12). Furthermore, 1 dnLGD variant was identified in 3625 trios by the Autism Sequencing Consortium (13). Moreover, in a large cohort of developmental disorders (DDs), 8 dnLGD variants and 6 de novo missense variants were identified from 31,058 DD parent-offspring trios (14). In this study, we identified 7 additional DNVs of *GIGYF1* from 7015 autism exome trios and performed a meta-analysis with previous studies to show that disruptions of *GIGYF1* are associated with NDD phenotypes, especially in autism.

GIGYF1 was originally identified as a binding partner to the tandem proline-rich region in the N-terminus of Grb10 in a yeast two-hybrid screening, and it was proposed to activate

ISSN: 0006-3223

IGF-1 (insulin-like growth factor 1) signaling (15). It was then found to repress target messenger RNA (mRNA) expression by interacting with 4EHP, which competes with eIF4E to bind to the 5′ cap structure of specific mRNAs (16,17). Moreover, GIGYF1 is reported to be involved in translation-coupled mRNA decay through binding with 4EHP (18). In *Drosophila*, *gyf* (homolog of *GIGYF1* and *GIGYF2*) was found to regulate autophagy (19). The null allele *gyf* flies exhibited shortened life span and impaired motor ability. Nevertheless, the role of *GIGYF1* in nervous system development remains poorly understood. Here, we generated zebrafish and mouse models of *GIGYF1* and found that the phenotypes observed in these models correlate well with the symptoms of patients carrying *GIGYF1* variants, establishing a causative relationship between *GIGYF1* mutations and neurodevelopmental defects.

METHODS AND MATERIALS

Animal Models

All animals were kept at standard temperature with controlled circadian cycle. The zebrafish mutant alleles were generated using CRISPR (clustered regularly interspaced short palindromic repeats)/Cas9 genome editing technology, as previously described (20). *Gigyf1* conditional knockout (cKO) mice were generated using the CRISPR/Cas9 system to flank the 10th–24th exons by loxP sites. Constitutive *Gigyf1* KO mice were generated by crossing cKO with CMV-Cre mice. All animal experiments were approved by the Animal Care and Use Committee of the animal core facility at Huazhong University of Science and Technology.

Behavioral Tests

All behavioral tests were performed using animals of the same age, sex, and housing conditions with littermate controls. Zebrafish larval adaptation assay, novel tank test, shoaling test, social behavior test, and mirror test were performed. Mice open field test, elevated plus maze, novel object recognition test, grooming test, marble burying test, T-maze, three-chamber sociability test, and fear conditioning test were performed at 6 to 10 weeks of age, according to standard protocols.

Transcriptomics

For zebrafish, heads of 4.3 days postfertilization (dpf) larvae were dissected, and total RNA was extracted for transcriptomic analyses. For mice, the cortex and hippocampus of postnatal day (P) 0 mice were dissected and used for bulk RNA sequencing. For single-nucleus RNA sequencing, hippocampi dissected from 6-week-old mice were used, followed by library preparation using the 10x Genomics Chromium Nuclei Isolation and Chromium Single Cell 3′ v3 pipeline. Sequencing was performed with Illumina NovaSeq6000.

Detailed methods, statistics statement, and data and code availability are provided.

RESULTS

Excess of De Novo *GIGYF1* Variants in Patients With NDDs

We first identified 7 DNVs (P1–P7, 3 dnLGD and 4 de novo missense variants) in *GIGYF1* from exome sequencing of 7015 trios with autism diagnosis from the SPARK project (21) and then integrated these with another 19 DNVs (P8–P26, 13 dnLGD and 6 de novo missense) from previously published cohorts with a primary diagnosis of ASD or DD (Table S1) (11–14,22). In all, we assembled a cohort of 26 DNVs in *GIGYF1* from a total of 44,665 unique NDD families (Table S2). The ratio of DNVs in ASD is ∼1.96-fold higher than that in DD cases (0.088% in ASD vs. 0.045% in DD, $p = .06$, one-sided Fisher's exact test) (Figure 1; Table S1). We re-evaluated the DNV enrichment for all genes using two statistical models: a modified chimpanzee-human divergence model (23) and the denovolyzeR (24) model. Both models identified a significant excess of dnLGD variants of *GIGYF1* in NDDs: modified chimpanzee-human divergence model ($p_{adj} = 4.62 \times 10^{-14}$, corrected by 18,946 genes tested) and denovolyzeR ($p_{adj} = 2.3 \times 10^{-16}$, corrected by 19,618 genes tested). These results confirmed that the DNVs in *GIGYF1* are significantly associated with NDDs.

Disruption of *GIGYF1* Is Associated With Autism and Other NDD Phenotypes

We were able to obtain detailed clinical information for 14 probands (P1–P14), whose average age at registration was 9.8 years (Table S3). Most probands were diagnosed with autism (85.7%, 12/14), and 83.3% (10/12) of cases exhibited behavioral abnormalities, such as social communication disorder, obsessive-compulsive disorder, social anxiety disorder, or social phobia. Speech delay and sleep disturbance (e.g., sleep disordered breathing, difficulty falling asleep, long and frequent naps, or nocturnal incontinence) commonly co-occurred. Dysmorphic facial features (27.3%, 3/11), such as hypertelorism, wide nasal bridge, or cleft palate, are usually seen in patients with DD, but not in autism cases, suggesting that it could be an indicator for more severe phenotypes. In addition, intellectual disability (35.7%, 5/14), motor delay (25%, 3/12), seizures (18.2%, 2/11), attention-deficit/hyperactivity disorder (18.2%, 2/11), hearing abnormalities (16.7%, 2/12), and cardiac anomalies (16.7%, 2/12) were also observed in subsets of the patients (Figure 1B). In summary, a wide range of ASD or NDD phenotypes are present in probands with DNVs in *GIGYF1*.

Generation of Zebrafish KO Alleles of *gigyf1*

There are 2 homologous genes of human *GIGYF1* in zebrafish, namely *gigyf1a* and *gigyf1b* (Figure S1A, B). We performed in situ hybridization and reverse transcriptase quantitative polymerase chain reaction to determine the temporospatial expression patterns of the 2 genes and found that they are both maternally and ubiquitously expressed during zygote cleavage, gastrulation, and epiboly and enriched in the head regions after 24 hours postfertilization (Figure S1C, D). We targeted the 2 genes using the CRISPR/Cas9 system and generated a 16-bp deletion allele for *gigyf1a* and a 4-bp deletion allele for *gigyf1b*, both of which introduce frameshifts and early truncations to the corresponding proteins (Figure 2A, B). We further performed Sanger sequencing, quantitative polymerase chain reaction and Western blotting to verify the KO effect of the mutant (Figure S1E–G). We subsequently crossed the homozygous single mutants and obtained homozygous *gigyf1a*; *gigyf1b* double mutants.

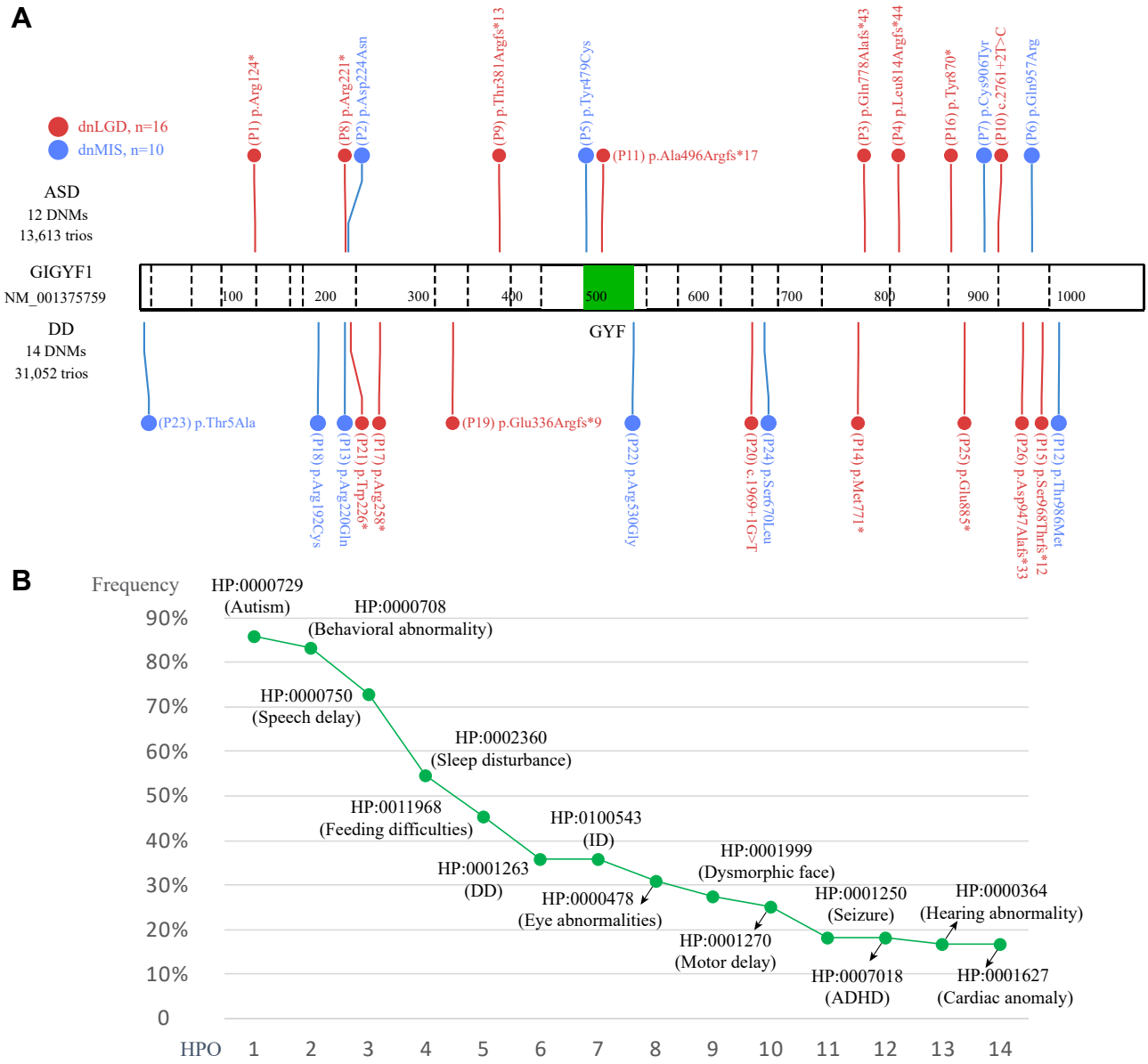

Figure 1. De novo variants in *GIGYF1* and the HPO frequencies. **(A)** dnLGD (red) and dnMIS (blue) variants in ASD (above) and DD (below) cohorts are depicted against a protein diagram for GIGYF1. The ASD and DD defined in this study refer to the primary diagnosis. GYF: domain contains conserved Gly-Tyr-Phe residues (middle green block). **(B)** The HPO phenotype frequencies were calculated only among the patients with phenotypic information available. Phenotypes with description available for <10 individuals were excluded from the calculation. ADHD, attention-deficit/hyperactivity disorder; ASD, autism spectrum disorder; DD, developmental disorder; dnLGD, de novo likely gene disruptive; dnMIS, de novo missense; DNV, de novo variant; HPO, human phenotype ontology; ID, intellectual disability.

Loss of *gigyf1a* and *gigyf1b* Leads to Developmental Defects in Zebrafish

To evaluate whether KO of *gigyf1a* and *gigyf1b* affects zebrafish development, we measured the body length and the distance between the convex tips of the eyes (interorbital distance, which is an indicator of brain size) (2). The overall embryonic development was not affected in any of the single mutants, except for a mild (~4%, $p = .006$) reduction of the interorbital distance in *gigyf1b*$^{-/-}$ (Figure S2). However, the body lengths of both 4.3-dpf double mutant larvae (~3%, $p < .001$) and 3-month-old adult fish (~9%, $p < .001$) were significantly reduced (Figure S3A–D). Moreover, the interorbital distance was further reduced (~10%, $p < .001$) in the double mutant compared with the *gigyf1b* single mutant (Figure S2G, H; Figure S3E, F). We further examined cell proliferation and apoptosis in the head region and observed that cell proliferation was significantly

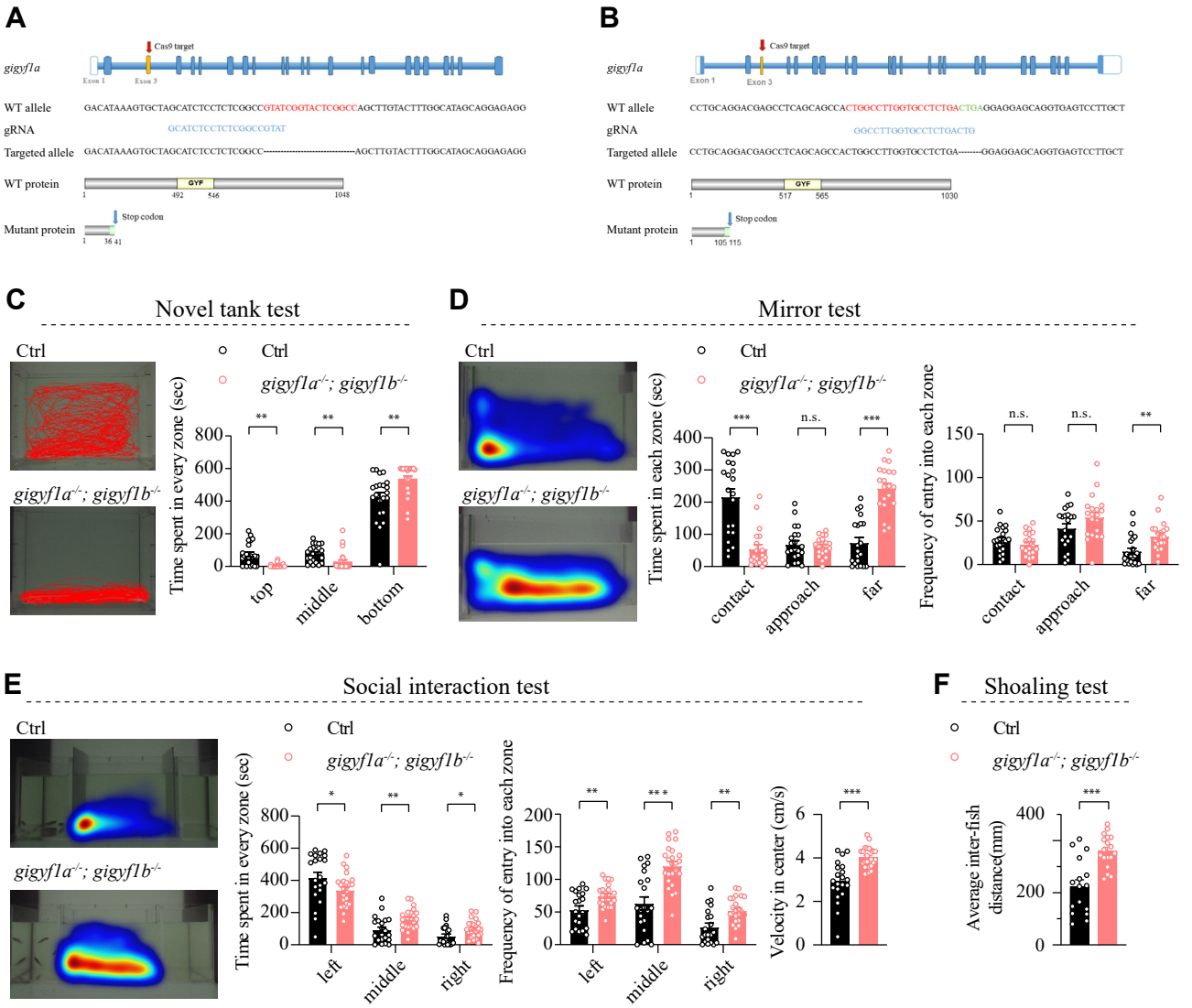

Figure 2. Knockout of zebrafish homologs of *GIGYF1* causes various behavioral defects. **(A, B)** Strategies for generating zebrafish *gigyf1a* and *gigyf1b* knockout alleles, respectively, using the CRISPR/Cas9 system. An allele with a 16-bp deletion in exon 3 of *gigyf1a* and an allele with a 4-bp deletion for *gigyf1b* were isolated. These alleles cause frameshift and early truncation for the proteins. The double mutant allele *gigyf1a*$^{-/-}$; *gigyf1b*$^{-/-}$ was then generated by crossing the single mutants. **(C)** In the novel tank test, *gigyf1a*$^{-/-}$; *gigyf1b*$^{-/-}$ mutants spent significantly reduced time in the top region and prolonged time in the bottom region. **(D)** In the mirror test, *gigyf1a*$^{-/-}$; *gigyf1b*$^{-/-}$ mutants were further away from the mirror than were the controls. **(E)** In the social interaction test, *gigyf1a*$^{-/-}$; *gigyf1b*$^{-/-}$ mutants exhibited reduced interest in the left chamber where other fishes were trapped. **(F)** The average distance between the *gigyf1a*$^{-/-}$; *gigyf1b*$^{-/-}$ mutants was greater than that of the controls in the shoaling test. Data in summary graphs are mean ± SEM; statistical comparisons were performed using Student's *t* test. n.s. $p > .05$; *$p < .05$; **$p < .01$; ***$p < .001$. CRISPR, clustered regularly interspaced short palindromic repeats; Ctrl, control; gRNA, guide RNA; n.s., nonsignificant; WT, wild-type.

reduced in the double mutants at 3 and 6 dpf and that apoptosis levels were elevated at 6 dpf (Figure S3G, H). The abnormal proliferation and apoptosis levels potentially contribute to the early embryonic developmental defects.

Loss of *gigyf1a* and *gigyf1b* Leads to Behavioral Defects Related to Human Patient Phenotypes

Next, we assessed the behaviors of the mutant. We performed an adaptation assay with repeated dark stimulation using 5-dpf larvae (Figure S4A). The initial responses were similar among all genotypes, and the control larvae exhibited gradually reduced responses after the second round of stimulation, whereas the *gigyf1a*$^{-/-}$; *gigyf1b*$^{-/-}$ larvae failed to adapt (Figure S4B–G). We then performed behavioral tests in adult fish (Figure S5). In the novel tank test, the mutants spent more time in the bottom region (Cohen's $d = -0.9180$, $p = .003$) and less time in the middle (Cohen's $d = 0.9973$, $p = .002$) or top (Cohen's $d = 1.0321$, $p = .001$) regions, indicating higher levels of anxiety (Figure 2C). In the mirror test, the mutants tended to move away from the reflection in the mirror (contact: Cohen's $d =$

1.7656, $p < .001$; approach: Cohen's $d = 0.1491$, $p = .638$; far: Cohen's $d = -2.2554$, $p < .001$), indicating reduced aggression levels (Figure 2D). In the three-chamber test, the mutants spent less time in the social area compared with the control group (left: Cohen's $d = 0.5937$, $p = .05$; middle: Cohen's $d = -0.9309$, $p = .003$; right: Cohen's $d = -0.7761$, $p = .013$), indicating attenuated social preference (Figure 2E). Moreover, the frequency of the fish entering into each zone (left: Cohen's $d = -0.9298$, $p = .003$; middle: Cohen's $d = -1.4640$, $p < .001$; right: Cohen's $d = -1.0774$, $p = .001$) and the average velocity (Cohen's $d = -1.4722$, $p < .001$) were increased in the mutants, again suggesting elevated anxiety levels (Figure 2E). Finally, in the shoaling test, the average distance among the mutants was significantly higher (Cohen's $d = -1.5669$, $p < .001$), indicating impaired social interactions (Figure 2F). In summary, loss of *gigyf1a* and *gigyf1b* in zebrafish led to defects in adaptation, aggression, anxiety, and social interaction behaviors.

Heterozygous KO of Mouse *Gigyf1* Results in Repetitive Behavior and Social Memory Deficits

To examine whether *GIGYF1* plays an evolutionarily conserved role, we also used mouse models. At P42, *Gigyf1* was detected at low levels in the spleen, liver, and kidney, but at high levels in the brain, spinal cord, lung, and heart (Figure 3A). Within the P42 brain, *Gigyf1* is expressed in various regions (Figure 3B; Figure S6A, B). Moreover, *Gigyf1* mRNA is highly expressed in the nervous system during various embryonic and postnatal periods (Figure 3C; Figure S6C).

We flanked the genomic region spanning from the 10th to the 24th exon of *Gigyf1* with loxP sites (Figure 3D). The loxP-flanked *Gigyf1* allele is referred to as a cKO allele. Consequently, we generated constitutive *Gigyf1* KO mice (Figure 3E). The homozygous *Gigyf1* KO mice died shortly after birth; therefore, we used the heterozygous *Gigyf1* KO (Het KO) mice for behavioral tests. The *Gigyf1* Het KO mice displayed repetitive behavior with excessive grooming (number of grooming bouts: Cohen's $d = -0.9229$, $p = .0394$; time spent grooming: Cohen's $d = -0.9451$, $p = .0353$) (Figure 3F). Locomotion activity was slightly decreased (Cohen's $d = 1.2988$, $p = .0031$), but anxiety levels in the open field were unchanged (Figure 3G). We then used the three-chamber social interaction assay to evaluate social behaviors. During the first phase, the sociability of *Gigyf1* Het KO mice was normal (Figure 3H). In the following phase, *Gigyf1* Het KO mice showed a significant deficit in the social novelty test (Cohen's $d = 0.8643$, $p = .0455$), also referred to as social memory (Figure 3I), suggesting a reduced ability to discriminate novel and familiar conspecifics. We did not detect significant changes in novel object recognition, rearing, marble burying, T-maze, or elevated plus maze (Figure 3J–N). Therefore, *Gigyf1* Het KO mice displayed increased repetitive behavior and decreased social memory, which are characteristics of ASD.

Conditional Ablation of *Gigyf1* in Excitatory Neurons Results in Repetitive Behavior and Social Memory Deficit

Using published datasets of single-cell RNA sequencing, we found that *Gigyf1* was widely expressed in distinct neuron types, especially the glutamatergic and GABAergic (gamma-aminobutyric acidergic) neurons in both cortices and the hippocampus (Figure S7A–C). To test the functions of *Gigyf1* in different types of neurons, we crossed the *Gigyf1* cKO mice with NEX-Cre and GAD2-Cre mice, respectively, which resulted in KO of *Gigyf1* in excitatory (e-cKO) or inhibitory (i-cKO) neurons (Figure 4A; Figure S7D, E). We performed Western blotting and quantitative polymerase chain reaction experiments and confirmed that both the protein and mRNA levels were significantly reduced in the cortical (protein: Cohen's $d = 14.7706$, $p < .001$; RNA: Cohen's $d = 36.3422$, $p < .001$) and hippocampal (protein: Cohen's $d = 2.7161$, $p = .0292$; RNA: Cohen's $d = 16.2511$, $p < .001$) regions of the *Gigyf1* e-cKO mice (Figure 4B, C; Figure S6D). We then evaluated the behavioral performances of the *Gigyf1* e-cKO and *Gigyf1* i-cKO mice using a series of behavioral tests. The *Gigyf1* e-cKO mice displayed repetitive behavior with excessive grooming (Cohen's $d = -0.7$, $p = .05$) (Figure 4D). However, we did not observe significant changes for the *Gigyf1* e-cKO mice in the open field, novel object recognition, rearing, marble burying, elevated plus maze, or fear conditioning tests (Figure 4E, F; Figure S6E, F, H–K). In the T-maze test, we detected a minor deficit in short-term memory for the *Gigyf1* e-cKO mice (Cohen's $d = 0.7804$, $p = .03$) (Figure S6G). In the three-chamber social interaction assay, the *Gigyf1* e-cKO mice showed a normal sociability (Figure 4G) but displayed a significant deficit in social memory (Cohen's $d = 1.3427$, $p < .001$) (Figure 4H). Therefore, the *Gigyf1* e-cKO mice phenocopied the increased repetitive behavior and decreased social memory observed in *Gigyf1* Het KO mice.

Interestingly, we observed different behavioral phenotypes in the *Gigyf1* i-cKO mice. These mice displayed reduced grooming behavior (Cohen's $d = 1.6758$, $p = .045$) (Figure 4I) and elevated anxiety levels (time in centers: Cohen's $d = 1.8695$, $p = .029$; velocity in centers: Cohen's $d = -2.5322$, $p = .004$) (Figure 4J), which were not observed in the *Gigyf1* e-cKO mice. We did not detect any significant changes in sociability, social novelty, learning and memory, or anxiety (Figure 4K, L, N–Q). However, *Gigyf1* i-cKO mice exhibited a significant impairment in cognitive performance in the novel object recognition test (Cohen's $d = 2.2221$, $p = .01$) (Figure 4M). In summary, these results showed a neuron type–specific role of *Gigyf1* in mouse behaviors.

GIGYF1 Regulates Downstream Target Genes Related to Neurodevelopment

To explore the molecular mechanisms by which *GIGYF1* regulates neurodevelopment, we performed transcriptomic and proteomic analyses in the 4.3-dpf zebrafish head tissues (Figure S8A–F). In total, we identified 1260 differentially expressed genes (DEGs) (461 downregulated and 799 upregulated) from the 20,553 detected genes in the transcriptomics data and 286 differentially expressed proteins (DEPs) (83 downregulated and 203 upregulated) from the 7848 proteins detected (Figure S9A, C; Table S4). The correlation between the DEGs and DEPs was poor, potentially due to differences in the detection range, sensitivity, and accuracy between the two methods (Figure S8G–I). Therefore, we analyzed gene functions for the two lists independently. To explore the functions of the downstream targets, we performed gene set enrichment analysis based on the fold change order of the DEGs and DEPs. The downregulated DEGs were mainly involved in the development of metencephalon, neuron, nerve, and dendritic

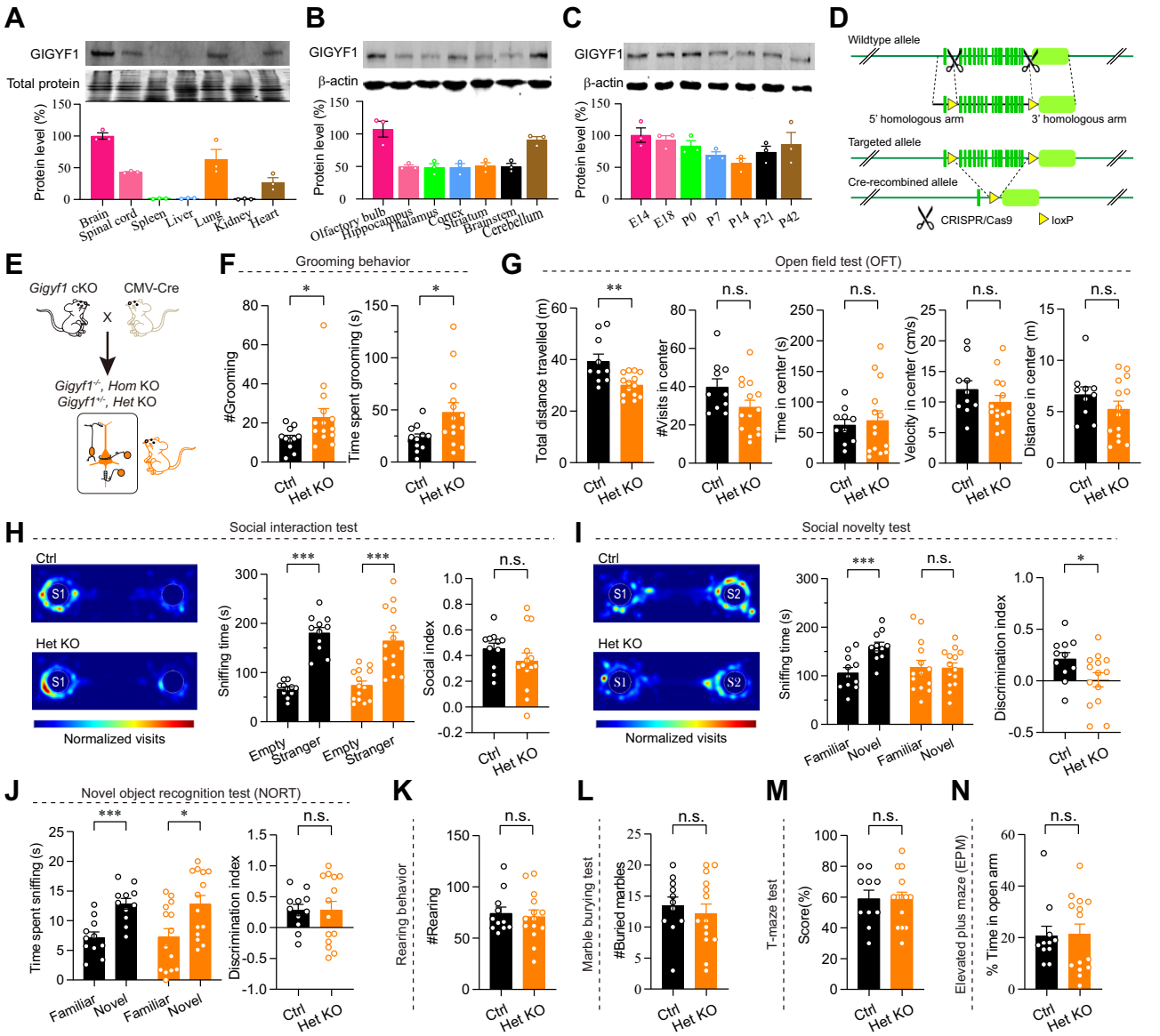

Figure 3. Haploinsufficiency of *Gigyf1* causes excessive repetitive behavior and impaired social memory. **(A)** Western blotting analysis of GIGYF1 protein levels in mouse brain, spinal cord, spleen, liver, lung, kidney, and heart at P42. Total protein was used as an internal control (n = 3). **(B)** Western blot analysis of GIGYF1 protein levels in the different brain regions (n = 3). **(C)** GIGYF1 protein levels in the developing mouse brain determined by Western blot (n = 3). **(D)** Targeting strategy for the generation of conditional *Gigyf1* KO mice in which the 10th through 24th exons were conditionally deleted by Cre recombinase. **(E)** *Gigyf1* is deleted by crossing *Gigyf1* cKO mice with CMV-cre mice. **(F)** The grooming bouts and duration are analyzed in control and *Gigyf1* Het KO mice, respectively (p = .0394 and .0353; control, n = 11; Het KO, n = 14). **(G)** Open field test reveals reduced locomotion in *Gigyf1* Het KO mice (p = .0031; control, n = 11; Het KO, n = 14). **(H)** During a social interaction session, *Gigyf1* Het KO mice have normal sociability. Left, position heat maps for the control and Het KO mice. Middle, sniffing time. Right, social index ($p > .05$; control, n = 11; Het KO, n = 14). **(I)** The same as **(H)** but for social novelty test. Left, position heat maps. Middle, sniffing time exploring S1 and S2. Right, social discrimination index (p = .0246; control, n = 11; Het KO, n = 14). **(J)** *Gigyf1* Het KO mice exhibit a normal recognition level in the novel object recognition test ($p > .05$; control, n = 11; Het KO, n = 14). **(K)** Rearing behavior. **(L)** Marble burying test. **(M)** T-maze test. **(N)** Elevated plus maze. Data in summary graphs are mean ± SEM; statistical comparisons were performed using Student's t test. n.s. $p > .05$; *$p < .05$; **$p < .01$; ***$p < .001$. cKO, conditional knockout; ctrl, control; Het, heterozygous; KO, knockout; n.s., nonsignificant; P42, postnatal day 42.

spine and the GABA signaling pathway (Figure S9B), whereas the DEPs were mainly involved in metabolic pathways and neurodegenerative diseases (Figure S9D). We then compared the DEGs and DEPs with the SFARI/DDD gene lists. Interestingly, a subset of the DEGs and DEPs are associated with different subtypes of NDDs (Figure S9E). Moreover, we annotated the gene-disease associations for the DEGs and DEPs using the DisGeNET database and found subsets of the

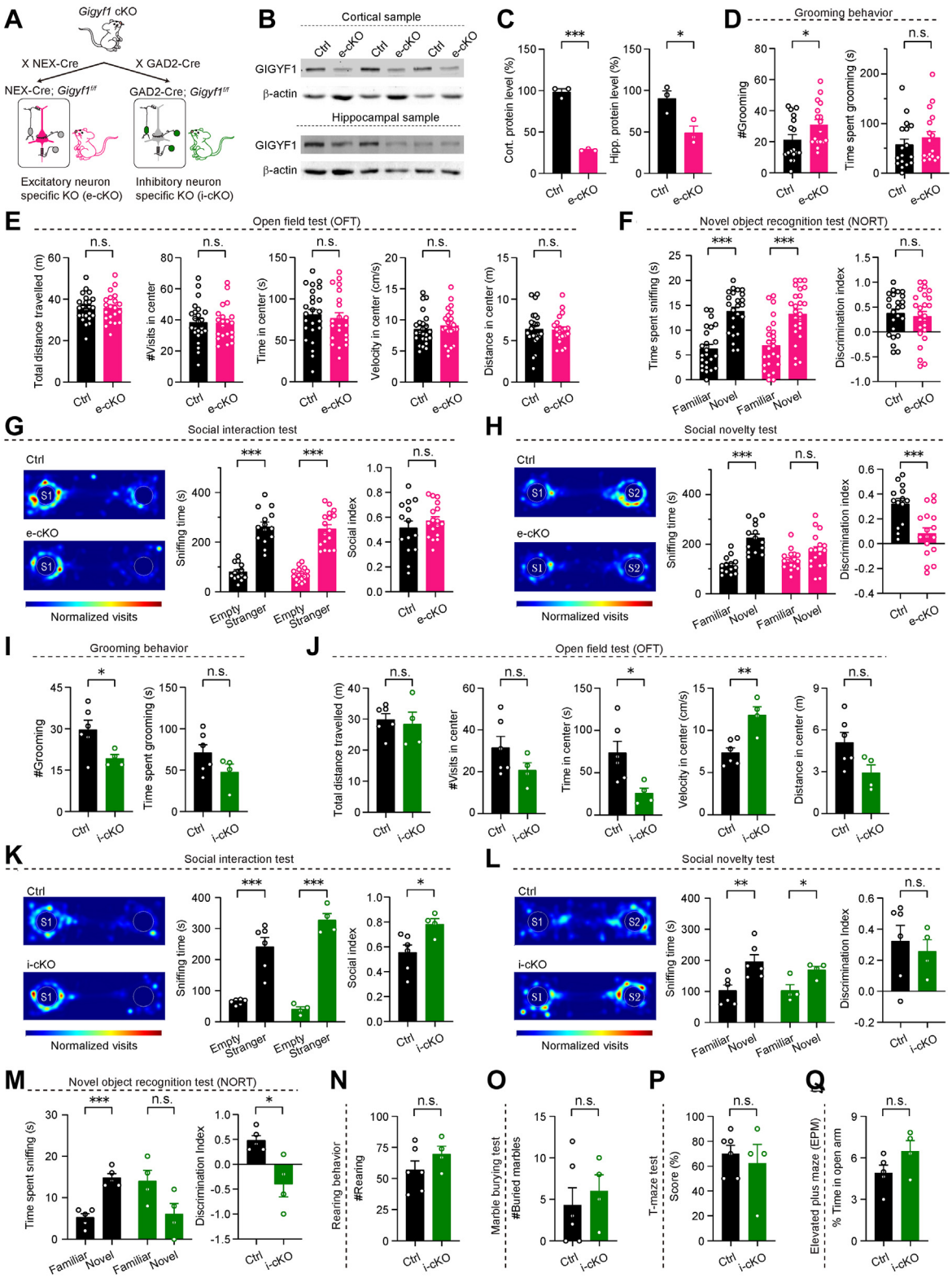

DEGs associated with intellectual disabilities, schizophrenia, depression, and autism, suggesting that these genes may be involved in the complex neurodevelopmental phenotypes associated with *GIGYF1* variants (Figure S9F).

Next, we performed bulk RNA sequencing in the hippocampus and cortex of mice at P0. Gene set enrichment analysis showed a significant downregulation in genes regulating synaptic structure and neurotransmitter transport (Figure S10A–D). To explore the conserved molecular pathways, we jointly analyzed the mRNA expression profiles of zebrafish and mouse KO models and identified 4 upregulated genes and 14 downregulated genes (Figure S10E, F). The downregulation of *Slc17a7*/VGLUT1 and *Grm2* suggests potential changes in glutamatergic synapses. Therefore, *GIGYF1* may regulate synaptic transmission in different species.

GIGYF1 Alters the Proportion of CA2 Glutamatergic Neurons

To further explore the neural mechanisms underlying the observed phenotypes, we performed immunohistochemistry on the hippocampus. The overall hippocampal architecture was normal in the *Gigyf1* Het KO mice (Figure S11A, B). The density of NeuN-positive neurons in the CA2 region was significantly increased (Cohen's $d = -1.4422$, $p = .0194$) (Figure S11A, B). We also performed immunostaining for VGLUT2 and GAD65/67. However, no significant change was observed, suggesting a normal synapse density (Figure S11C–F).

Next, we performed single-nucleus RNA sequencing in the hippocampus to examine the role of *Gigyf1* in different populations of neurons. We analyzed the transcriptomes of 16,211 cells (control: 5965 and Het KO: 10,246) and identified 9 major clusters (Figure 5A). We further clustered the neurons into 9 subpopulations (Figure 5B, C). Importantly, the *Gigyf1* Het KO mice harbored a higher percentage of *Slc17a7*$^+$ (*Vglut1*$^+$) excitatory neurons in the CA2-CA3 region (Figure 5D), correlating with the increased neuron density in the CA2 region observed by NeuN staining (Figure S11A, B). We further explored the transcriptomic changes in the major glutamatergic neurons. The four clusters of neurons shared a common upregulated gene, *Xist*, and a downregulated gene, *Nr3c2* (Figure 5E). The significantly downregulated genes are involved in various processes related to neuronal function, including presynaptic and postsynaptic structures, neurotransmitter transport, membrane potential, ion channel, and glutamate receptor activity (Figure 5F, G). In the single-cell pseudotime trajectory analysis, neurons in different hippocampal subfields showed distinct differentiation paths originating from neuroblasts (Figure S12A, B). We further identified the key DEGs of the differentiation node, many of which were also differentially expressed between control and Het KO groups (Figure S12C). These results indicate that haploinsufficiency of *Gigyf1* leads to increased CA2 glutamatergic neurons and synaptic dysfunctions, which may contribute to autism-like behaviors by inducing excitatory/inhibitory imbalance.

DISCUSSION

In this study, we integrated 26 DNVs in *GIGYF1* from a large cohort with 44,665 NDD trios, which includes 13,613 trios with a primary diagnosis of ASD and 31,052 trios with DD. Notably, we included well-known cohorts with underlying sequencing reads for reanalysis and/or detailed clinical records for phenotypic comparison, which should stand as a good representative set of NDD cohorts. We also want to note that the ASD and DD used and defined in this study refer to primary diagnosis; therefore, there may be overlap of symptoms between ASD and DD because it has been well reported that patients with differently diagnosed NDD sometimes have overlapping phenotypes (25,26). The patients carrying *GIGYF1* variants exhibit very similar phenotypes, strongly suggesting that variants of *GIGYF1* are probably the genetic causes of the disease. To further establish a causal relationship, we generated zebrafish and mouse models and demonstrated that loss of *Gigyf1* leads to developmental and behavioral defects that correlate with human phenotypes in both models.

In zebrafish mutants, the reduced body length in larval stage correlates with the global developmental delay in patients. The reduced interorbital distance and dysregulation of proliferation/apoptosis in zebrafish larvae potentially correspond to the microcephaly and dysmorphic face phenotypes. The

Figure 4. Deletion of *Gigyf1* in excitatory neurons and inhibitory neurons results in differential behavioral deficits in repetitive behavior, social memory, anxiety, and cognition. **(A)** *Gigyf1* is conditionally deleted in excitatory neurons (*Gigyf1* e-cKO) and inhibitory neurons (*Gigyf1* i-cKO), respectively. **(B)** Western blot of cortical (left) and hippocampal (right) lysate from control and *Gigyf1* e-cKO mice. **(C)** Summary graphs showing that GIGYF1 protein levels are decreased in *Gigyf1* e-cKO mice (cortical KO = 31.86% ± 0.81%, $n = 3$, $p < .001$; hippocampal KO = 55.87% ± 6.46%, $n = 3$, $p = .003$). Values are normalized and compared with the WT. **(D)** The grooming bouts and duration are analyzed in *Gigyf1* e-cKO, respectively ($p = .0496$ and .4066; control, $n = 17$; e-cKO, $n = 17$). **(E)** The open field test suggests anxiety level is not changed in *Gigyf1* e-cKO mice ($p > .05$; control, $n = 24$; e-cKO, $n = 21$). **(F)** *Gigyf1* e-cKO mice exhibit a normal recognition level in the novel object recognition test ($p > .05$; control, $n = 24$; e-cKO, $n = 25$). **(G)** During the social interaction session, *Gigyf1* e-cKO mice have normal sociability. Left, position heat maps for the control and *Gigyf1* e-cKO mice exploring the pencil cups with or without stranger 1 (S1). Middle, the sniffing time the subject mice spent in the circle (20 cm in diameter) surrounding the pencil cup, which is empty or has a stranger (S1) in it. Right, social index ($p > .05$; control, $n = 14$; e-cKO, $n = 17$). **(H)** Same as **(G)** but for social novelty test. Left, position heat maps. Middle, the sniffing time exploring stranger 1 (familiar stranger, S1) and stranger 2 (novel stranger, S2). Right, social discrimination index ($p = .0009$; control, $n = 14$; e-cKO, $n = 17$). **(I)** The grooming bouts and duration, respectively, are analyzed in *Gigyf1* i-cKO ($p = .0451$ and .1522; control, $n = 6$; i-cKO, $n = 4$). **(J)** Open field test suggests anxiety level is elevated in *Gigyf1* i-cKO mice ($p > .05$; control, $n = 6$; i-cKO, $n = 4$). **(K)** During the social interaction session, *Gigyf1* i-cKO mice have normal sociability. Left, position heat maps for the control and *Gigyf1* i-cKO mice. Middle, sniffing time. Right, social index ($p > .05$; control, $n = 6$; i-cKO, $n = 4$). **(L)** The same as **(K)** but for social novelty test. Left, position heat maps. Middle, sniffing time exploring S1 and S2. Right, social discrimination index ($p > .05$; control, $n = 6$; i-cKO, $n = 4$). **(M)** *Gigyf1* i-cKO mice exhibit impaired recognition level in the novel object recognition test ($p = .0101$; control, $n = 5$; i-cKO, $n = 4$). **(N)** Rearing behavior. **(O)** Marble burying test. **(P)**, T-maze test. **(Q)** Elevated plus maze. Data in summary graphs are mean ± SEM; statistical comparisons were performed using Student's *t* test. n.s. $p > .05$; *$p < .05$; **$p < .01$; ***$p < .001$. cKO, conditional KO; cort., cortical; Ctrl, control; CRISPR, clustered regularly interspaced short palindromic repeats; Het, heterozygous; Hipp., hippocampal; Hom, homozygous; KO, knockout; n.s., nonsignificant; WT, wild-type.

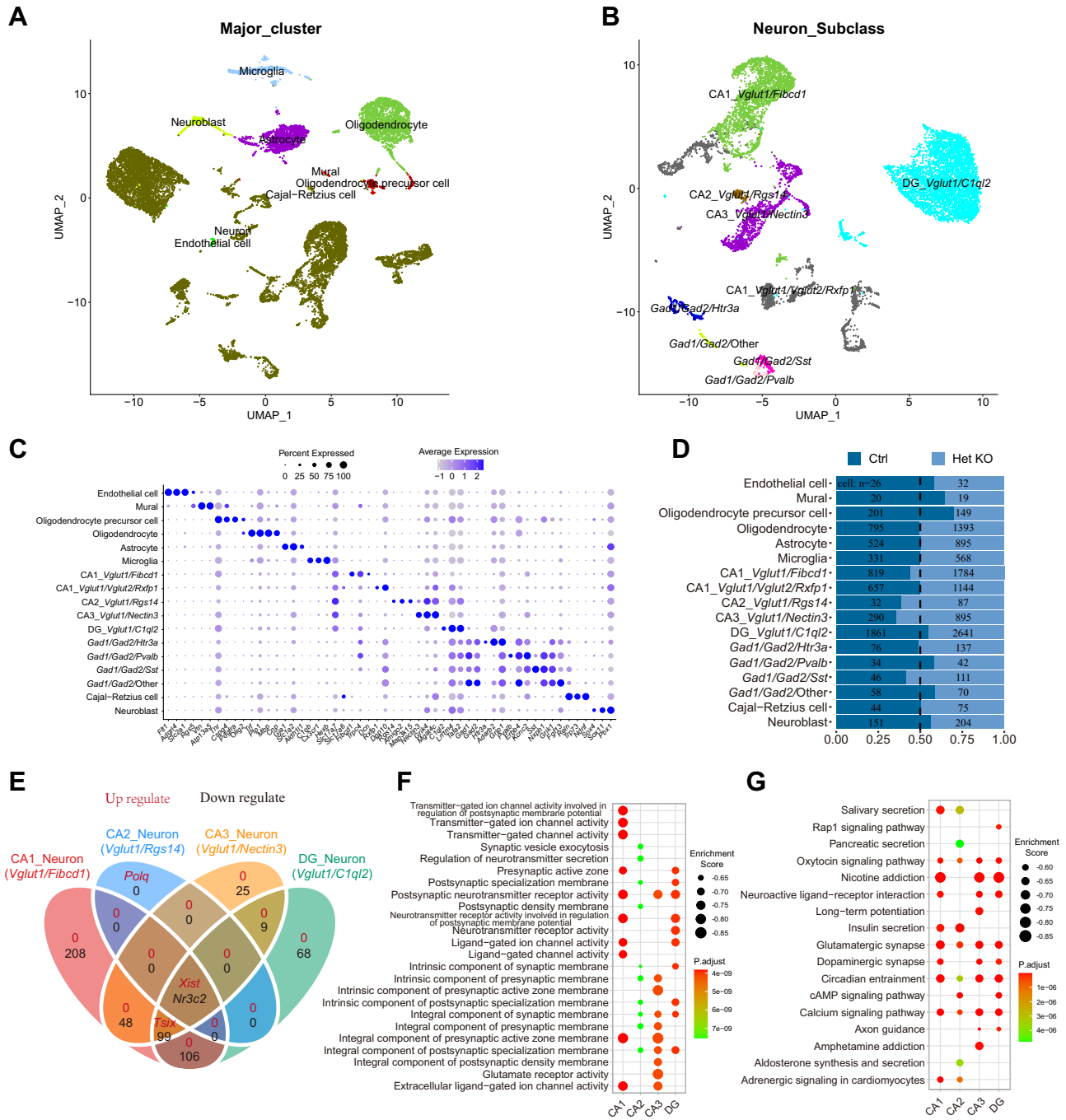

Figure 5. Single-nucleus RNA sequencing of hippocampus from P42 *Gigyf1* Het KO mice. **(A)** UMAP of hippocampal cells of *Gigyf1* Het KO and control mice, which were clustered into 9 major cell types. **(B)** The hippocampal neurons from *Gigyf1* Het KO and control mice were clustered into 9 neuronal subpopulations, including 5 classes of excitatory neurons and 4 classes of inhibitory neurons. **(C)** Dot plots showing molecular signatures of clusters from panels **(A)** and **(B)**. The percentage of cells expressing the gene (circle size) and average gene expression level (color scale) are displayed. **(D)** Relative proportions and number of cells in the clusters between the *Gigyf1* Het KO and control samples. **(E)** The intersections of differentially expressed genes among clusters of CA1_*Vglut1/Fibcd1*, CA2_*Vglut1/Rgs14*, CA3_*Vglut1/Nectin3*, and DG_*Vglut1/C1ql2*. Differential expression analyses were performed between the *Gigyf1* Het KO and the control group (upregulated genes in red and downregulated genes in black). **(F)** Gene set enrichment analysis of CA1_*Vglut1/Fibcd1*, CA2_*Vglut1/Rgs14*, CA3_*Vglut1/Nectin3*, and DG_*Vglut1/C1ql2* clusters based on the Gene Ontology database. **(G)** Gene set enrichment analysis of CA1_*Vglut1/Fibcd1*, CA2_*Vglut1/Rgs14*, CA3_*Vglut1/Nectin3*, and DG_*Vglut1/C1ql2* clusters based on the Kyoto Encyclopedia of Genes and Genomes PATHWAY database. cAMP, cyclic adenosine monophosphate; Ctrl, control; DG, dentate gyrus; Het KO, heterozygous knockout; P42, postnatal day 42; UMAP, uniform manifold approximation and projection.

behavioral phenotypes, including adaptation defects, elevated anxiety levels, reduced aggression, and impaired social preference, have all been widely considered key features of ASD-related animal models that reflect the behavioral abnormalities in humans. The zebrafish model thus successfully recapitulates many aspects of the phenotypes of patients carrying loss-of-function mutations in *GIGYF1*.

We also systematically evaluated behavioral phenotypes in *Gigyf1* Het KO, *Gigyf1* e-cKO, and *Gigyf1* i-cKO mice and detected convergent behavioral deficits, including repetitive behaviors and social dysfunction. We found that deletion of *Gigyf1* in excitatory neurons increases repetitive behavior and impairs social memory, while loss of *Gigyf1* in inhibitory neurons increases anxiety level and impairs cognition. These findings in mice extend the observations in zebrafish, providing insights into the functions of *Gigyf1* in different neuronal subtypes. Previous studies showed that anxiety regulation is related to multiple brain regions, including the medial prefrontal cortex, lateral septum, nucleus accumbens, central amygdala, basolateral amygdala, ventral tegmental area, and hippocampus (27). Some of these regions (i.e., lateral septum, nucleus accumbens, central amygdala) mainly include GABAergic neurons, while others include both excitatory and inhibitory neurons. Therefore, *Gigyf1* may regulate anxiety levels mainly through GABAergic neurons. It has been suggested that repetitive behaviors may be related to an imbalance of direct and indirect pathways in the basal ganglion (28–30). Notably, we detected elevated repetitive behavior in *Gigyf1* e-cKO mice, suggesting that *GIGYF1* in glutamatergic neurons may play a role in regulating the function of the basal ganglion. Social behaviors are a series of social interactions between subject mouse and conspecifics, which involve continuous integration of multiple types of information, including acute sensory inputs, internal social state, previous social experience retrieval, and decision making (31). Here, we consistently observed a social memory deficit in both *Gigyf1* Het KO and *Gigyf1* e-cKO but not in *Gigyf1* i-cKO mice. It has been shown that the hippocampal CA2 region and upstream inputs play crucial roles in social memory encoding (32–35). Here, we detected an increased number of pyramidal neurons in the hippocampal CA2 region. Moreover, the single-nucleus RNA sequencing results also indicate increased excitatory neuronal populations in the CA2 region. Therefore, the increased CA2 neurons may be responsible for the observed behavioral deficits.

One potential caveat is that NEX-Cre and GAD2-Cre mice may not have the exact same genetic background, which may introduce some noise in neurobehavioral research (36). It has been shown that brain weight, locomotor activity, and ethanol preference in the same mouse strain were relatively stable in experiments performed in different laboratories across ~30 years (37). However, anxiety-related behaviors were highly variable across different laboratories, times, and even locations (37). Therefore, it is crucial to use littermate control and KO animals, which ensure the same sex, age, housing conditions, and genetic background in neurobehavioral studies.

The second caveat is that distinct DNVs in *GIGYF1* observed in human patients may lead to early-stop, missense, or frameshift mutations, and each mutation may represent a unique subtype of *GIGYF1*-related NDD. Here, we used *GIGYF1* KO zebrafish or mouse models, which may only mimic the loss-of-function mutations observed in human patients. It is highly possible that different *GIGYF1* DNVs may result in different structural and functional deficits, which are similar to other subtypes of *GIGYF1*-related disorders.

We also examined whether GIGYF1 is involved in gene regulation in the developing brain by transcriptomic and proteomic analyses. We identified more than a thousand potential targets of GIGYF1, many of which have been associated with different aspects of neurodevelopment and subtypes of NDDs (38,39). Interestingly, in *GIGYF1* KO models of both species, synaptic protein expression was significantly disturbed (Figure 5F, G), suggesting an important role of *GIGYF1* in regulating synaptic functions.

In summary, our findings establish the relationship between variants in *GIGYF1* and neurodevelopmental defects and help to establish the neuronal foundation for understanding the precise molecular mechanisms underlying clinical phenotypes related to *GIGYF1* loss-of-function mutations.

ACKNOWLEDGMENTS AND DISCLOSURES

This work was supported, in part, by grants from the National Natural Science Foundation of China (Grant Nos. 81671118 and 81721005 [to BX], 31871028 and 32271197 [to MJ], and 82201314 [to TW]), the U.S. National Institutes of Health (Grant Nos. R01MH101221 and U01MH119705 [to EEE]), the Simons Foundation Autism Research Initiative (Grant No. 608045 [to EEE]), and the Fundamental Research Funds for the Central Universities starting fund (Grant No. BMU2022RCZX038 [to TW]). EEE is an investigator of the Howard Hughes Medical Institute.

We acknowledge the support from the National Institute for Health Research through the Comprehensive Clinical Research Network. We thank Tonia Brown for assistance in editing this manuscript. We are grateful to the SPARK Consortium for granting access to the exome sequencing data.

EEE is on the scientific advisory board of Variant Bio, Inc. All other authors report no biomedical financial interests or potential conflicts of interest.

ARTICLE INFORMATION

From the Department of Forensic Medicine, Tongji Medical College, Huazhong University of Science and Technology, Wuhan, Hubei, China (ZD, WD, HJ, ZY, KW, XC, BX); Department of Pathology, School of Basic Medicine, Anhui Medical University, Hefei, Anhui, China (ZD); Department of Neurobiology, School of Basic Medicine, Tongji Medical College, Huazhong University of Science and Technology, Wuhan, Hubei, China (GH, YH); Department of Medical Genetics, Center for Medical Genetics, Peking University Health Science Center, Beijing, China (TW); Neuroscience Research Institute, Peking University, Key Laboratory for Neuroscience, Ministry of Education of China & National Health Commission of China, Beijing, China (TW); Department of Genome Sciences, University of Washington School of Medicine, Seattle, Washington (TW, EEE); Department of Physiology, School of Basic Medicine, Tongji Medical College, Huazhong University of Science and Technology, Wuhan, Hubei, China (HL, YW, MJ); Department of Psychiatry & Behavioral Sciences, University of Washington, Seattle, Washington (ECK-N, KA, RKE); Simons Foundation, New York (PF, WKC); Department of Pediatrics, Columbia University, New York (WKC); and Howard Hughes Medical Institute, University of Washington, Seattle, Washington (EEE).

ZD, GH, and TW contributed equally to this work.

KA is currently affiliated with the Department of Psychiatry, Geisel School of Medicine at Dartmouth, Dartmouth Hitchcock Medical Center, Lebanon, NH.

Address correspondence to Man Jiang, Ph.D., at manjiang@hust.edu.cn, or Bo Xiong, Ph.D., at bxiong@hust.edu.cn.

Received Jun 3, 2022; revised Feb 1, 2023; accepted Feb 16, 2023.

Supplementary material cited in this article is available online at https://doi.org/10.1016/j.biopsych.2023.02.993.

REFERENCES

1. Lai M-C, Lombardo MV, Baron-Cohen S (2014): Autism. Lancet 383:896–910.
2. Bernier R, Golzio C, Xiong B, Stessman HA, Coe BP, Penn O, *et al.* (2014): Disruptive CHD8 mutations define a subtype of autism early in development. Cell 158:263–276.
3. Stessman HAF, Willemsen MH, Fenckova M, Penn O, Hoischen A, Xiong B, *et al.* (2016): Disruption of POGZ is associated with intellectual disability and autism spectrum disorders. Am J Hum Genet 98:541–552.
4. Maenner MJ, Shaw KA, Baio J, EdS1, Washington A, Patrick M, *et al.* (2020): Prevalence of autism spectrum disorder among children aged 8 years – Autism and developmental disabilities monitoring network, 11 sites, United States, 2016. MMWR Surveill Summ 69:1–12.
5. Xu G, Strathearn L, Liu B, Bao W (2018): Prevalence of autism spectrum disorder among US children and adolescents, 2014-2016. JAMA 319:81–82.
6. De Rubeis S, Buxbaum JD (2015): Genetics and genomics of autism spectrum disorder: Embracing complexity. Hum Mol Genet 24:R24–R31.
7. Bai D, Yip BHK, Windham GC, Sourander A, Francis R, Yoffe R, *et al.* (2019): Association of genetic and environmental factors with autism in a 5-country cohort. JAMA Psychiatry 76:1035–1043.
8. Iossifov I, O'Roak BJ, Sanders SJ, Ronemus M, Krumm N, Levy D, *et al.* (2014): The contribution of de novo coding mutations to autism spectrum disorder. Nature 515:216–221.
9. Ruzzo EK, Pérez-Cano L, Jung JY, Wang LK, Kashef-Haghighi D, Hartl C, *et al.* (2019): Inherited and de novo genetic risk for autism impacts shared networks. Cell 178:850–866.e26.
10. Turner TN, Coe BP, Dickel DE, Hoekzema K, Nelson BJ, Zody MC, *et al.* (2017): Genomic patterns of de novo mutation in simplex autism. Cell 171:710–722.e12.
11. Krumm N, Turner TN, Baker C, Vives L, Mohajeri K, Witherspoon K, *et al.* (2015): Excess of rare, inherited truncating mutations in autism. Nat Genet 47:582–588.
12. Feliciano P, Zhou X, Astrovskaya I, Turner TN, Wang T, Brueggeman L, *et al.* (2019): Exome sequencing of 457 autism families recruited online provides evidence for autism risk genes. NPJ Genom Med 4:19.
13. Satterstrom FK, Kosmicki JA, Wang J, Breen MS, De Rubeis S, An JY, *et al.* (2020): Large-scale exome sequencing study implicates both developmental and functional changes in the neurobiology of autism. Cell 180:568–584.e23.
14. Kaplanis J, Samocha KE, Wiel L, Zhang Z, Arvai KJ, Eberhardt RY, *et al.* (2020): Evidence for 28 genetic disorders discovered by combining healthcare and research data. Nature 586:757–762.
15. Giovannone B, Lee E, Laviola L, Giorgino F, Cleveland KA, Smith RJ (2003): Two novel proteins that are linked to insulin-like growth factor (IGF-I) receptors by the Grb10 adapter and modulate IGF-I signaling. J Biol Chem 278:31564–31573.
16. Amaya Ramirez CC, Hubbe P, Mandel N, Béthune J (2018): 4EHP-independent repression of endogenous mRNAs by the RNA-binding protein GIGYF2. Nucleic Acids Res 46:5792–5808.
17. Peter D, Weber R, Sandmeir F, Wohlbold L, Helms S, Bawankar P, *et al.* (2017): GIGYF1/2 proteins use auxiliary sequences to selectively bind to 4EHP and repress target mRNA expression. Genes Dev 31:1147–1161.
18. Weber R, Chung MY, Keskeny C, Zinnall U, Landthaler M, Valkov E, *et al.* (2020): 4EHP and GIGYF1/2 mediate translation-coupled messenger RNA decay. Cell Rep 33:108262.
19. Kim M, Semple I, Kim B, Kiers A, Nam S, Park HW, *et al.* (2015): Drosophila Gyf/GRB10 interacting GYF protein is an autophagy regulator that controls neuron and muscle homeostasis. Autophagy 11:1358–1372.
20. Moravec CE, Pelegri FJ (2019): An accessible protocol for the generation of CRISPR-Cas9 knockouts using INDELs in zebrafish. Methods Mol Biol 1920:377–392.
21. Zhou X, Feliciano P, Shu C, Wang T, Astrovskaya I, Hall JB, *et al.* (2022): Integrating de novo and inherited variants in 42,607 autism cases identifies mutations in new moderate-risk genes. Nat Genet 54:1305–1319.
22. Deciphering Developmental Disorders Study (2017): Prevalence and architecture of de novo mutations in developmental disorders. Nature 542:433–438.
23. Wang T, Guo H, Xiong B, Stessman HAF, Wu H, Coe BP, *et al.* (2016): De novo genic mutations among a Chinese autism spectrum disorder cohort. Nat Commun 7:13316.
24. Samocha KE, Robinson EB, Sanders SJ, Stevens C, Sabo A, McGrath LM, *et al.* (2014): A framework for the interpretation of de novo mutation in human disease. Nat Genet 46:944–950.
25. Matson JL, Shoemaker M (2009): Intellectual disability and its relationship to autism spectrum disorders. Res Dev Disabil 30:1107–1114.
26. Wang T, Kim CN, Bakken TE, Gillentine MA, Henning B, Mao Y, *et al.* (2022): Integrated gene analyses of de novo variants from 46,612 trios with autism and developmental disorders. Proc Natl Acad Sci USA 119:e2203491119.
27. Calhoon GG, Tye KM (2015): Resolving the neural circuits of anxiety. Nat Neurosci 18:1394–1404.
28. DiCarlo GE, Aguilar JI, Matthies HJ, Harrison FE, Bundschuh KE, West A, *et al.* (2019): Autism-linked dopamine transporter mutation alters striatal dopamine neurotransmission and dopamine-dependent behaviors. J Clin Invest 129:3407–3419.
29. Pavăl D (2017): A dopamine hypothesis of autism spectrum disorder. Dev Neurosci 39:355–360.
30. Tecuapetla F, Matias S, Dugue GP, Mainen ZF, Costa RM (2014): Balanced activity in basal ganglia projection pathways is critical for contraversive movements. Nat Commun 5:4315.
31. Chen P, Hong W (2018): Neural circuit mechanisms of social behavior. Neuron 98:16–30.
32. Hitti FL, Siegelbaum SA (2014): The hippocampal CA2 region is essential for social memory. Nature 508:88–92.
33. Oliva A, Fernández-Ruiz A, Leroy F, Siegelbaum SA (2020): Hippocampal CA2 sharp-wave ripples reactivate and promote social memory. Nature 587:264–269.
34. Pimpinella D, Mastrorilli V, Giorgi C, Coemans S, Lecca S, Lalive AL, *et al.* (2021): Septal cholinergic input to CA2 hippocampal region controls social novelty discrimination via nicotinic receptor-mediated disinhibition. eLife 10:e65580.
35. Wu X, Morishita W, Beier KT, Heifets BD, Malenka RC (2021): 5-HT modulation of a medial septal circuit tunes social memory stability. Nature 599:96–101.
36. Matsuo N, Takao K, Nakanishi K, Yamasaki N, Tanda K, Miyakawa T (2010): Behavioral profiles of three C57BL/6 substrains. Front Behav Neurosci 4:29.
37. Wahlsten D, Bachmanov A, Finn DA, Crabbe JC (2006): Stability of inbred mouse strain differences in behavior and brain size between laboratories and across decades. Proc Natl Acad Sci U S A 103:16364–16369.
38. Li X, Zhang K, He X, Zhou J, Jin C, Shen L, *et al.* (2021): Structural, functional, and molecular imaging of autism spectrum disorder. Neurosci Bull 37:1051–1071.
39. Parenti I, Rabaneda LG, Schoen H, Novarino G (2020): Neurodevelopmental disorders: From genetics to functional pathways. Trends Neurosci 43:608–621.